Steroid hormones stimulate human prostate cancer progression and metastasis

**William A. Ricke[1], Kenichiro Ishii[2], Emily A. Ricke[1], Jeff Simko[3], Yuzhuo Wang[4], Simon W. Hayward[2]
and Gerald R. Cunha[1]***

[1]*Department of Anatomy, University of California, San Francisco, CA*
[2]*Department of Urologic Surgery, Vanderbilt University Medical Center, A1302, Medical Center North, Nashville, TN*
[3]*Department of Anatomic Pathology, University of California, San Francisco, CA*
[4]*Department of Cancer Endocrinology, BC Cancer Agency, Vancouver, BC V5Z 1L3, Canada*

Tissue recombinants (TRs) composed of mouse urogenital mesenchyme (mUGM) plus an immortalized nontumorigenic human prostatic epithelial cell line (BPH-1) were grown under the kidney capsule of male athymic nude mice under different hormonal conditions. The objectives were to determine temporal plasma concentrations of testosterone (T) and estradiol-17β (E_2) that elicit progression of nontumorigenic human prostatic epithelial cells *in vivo*. Second, to determine whether mUGM+BPH-1 TRs in [T+E_2]-treated hosts could progress to metastases. Control mouse hosts received no exogenous hormonal support, whereas treated mice received Silastic implants containing T and E_2 for 1–4 months. Plasma from hormonally treated mice contained significantly higher ($p < 0.01$) concentrations of T at 1 month (11.7 *vs.* 0.9 ng/ml). Plasma levels of E_2 in steroid implanted mice were significantly higher ($p < 0.05$) at 2 months (104.5 *vs.* 25.6 ng/l) and 4 months (122.8 *vs.* 19.2 pg/ml). Wet weights of mUGM+BPH-1 TRs from [T+E_2]-implanted mice were significantly larger ($p < 0.001$) than those from untreated hosts. Untreated mUGM+BPH-1 TRs contained a well organized differentiated epithelium surrounded by smooth muscle stroma similar to developing prostate. In [T+E_2]-implanted mice, mUGM+BPH-1 TRs formed carcinomas that contained a fibrous connective tissue stroma permeating the tumor; smooth muscle when present was associated with vasculature. Renal lymph nodes collected from [T+E_2]-treated mice, but not untreated mice, contained metastatic carcinoma cells. Moreover, metastases could be observed at distant sites including lung and liver. Epithelial cells isolated from untreated mUGM+BPH-1 TRs exhibited benign histology and formed small nontumorigenic grafts when subsequently transplanted into athymic nude mice. In contrast, epithelial cells isolated from mUGM+BPH-1 tumors of [T+E_2]-treated hosts formed large tumors that grew independent of stromal and hormonal support and developed lymph node metastases. We conclude that [T+E_2]-treatment promotes prostatic cancer progression in mUGM + BPH-1 TRs. Use of mUGM in this system will allow future studies to utilize the power of mouse genetics to identify paracrine factors involved in human prostatic carcinogenesis.
© *2005 Wiley-Liss, Inc.*

Prostate cancer (PRCA) has been detected in over 230,000 men in the United States in 2004. Many of these patients will undergo treatment to halt or slow PRCA progression. Many more will be diagnosed with advanced PRCA for which there is no cure. Moreover, this year more than 30,000 men will die of this disease. Goals of early detection, surgery, hormone therapy and chemoprevention are to decrease morbidity and mortality and increase life span. To achieve these goals, useful models of human PRCA progression must be developed.

Sex steroids are known to play important roles in prostatic carcinogenesis. In men and dogs, levels of serum androgens decrease with age, whereas estradiol-17β (E_2) increases. Accordingly, the E_2 to androgen ratio increases during the period when PRCA is detected in men.[1] E_2 in combination with testosterone (T) has been shown to induce carcinogenesis in rats and mice.[2–7] These models support the hypothesis that changes in hormonal milieu are not only implicated in PRCA but may be causal. Although animal models of hormone-induced PRCA demonstrate a natural progression *in vivo*, they have a low penetrance,[8] long latency[4] and do not

metastasize to distant organs.[2,9] Determining how T and E_2 stimulate prostatic carcinogenesis will elucidate mechanisms of disease progression and may lead to better therapeutics.

The prostate is a target organ for both E_2 and T. Estrogen is a prostatic mitogen. Long-term chronic treatment with estrogens elicits squamous metaplasia of prostatic epithelium.[10] Estrogenic effects in the prostate are mediated *via* estrogen receptors (ER) α and β. These receptors are found within the prostate primarily in stroma and epithelium, respectively.[11–14] Detection of ER-α within the epithelium is rare and typically found only within metastases.[15] Epithelial ER-β expression is usually decreased as tumors progress and may increase as metastatic cells encounter different stromal microenvironments.[15]

Androgens regulate prostatic development, growth and function, and are required for prostatic tumorigenesis. Androgenic effects are mediated *via* androgen receptors (AR) expressed in both epithelium and stroma. The respective roles of epithelial *versus* stromal AR in prostatic development, growth and function have been elucidated by analysis of tissue recombinants (TRs) composed of AR-positive wild-type and AR-negative testicular feminization mouse epithelium and stroma.[16] Prostatic epithelial development and growth are elicited *via* signaling through stromal AR.[17] Production of epithelial androgen-dependent secretory proteins is dependent upon epithelial AR.[18] The respective roles of epithelial *versus* stromal AR and ER in prostatic carcinogenesis remains to be elucidated.

Stromal factors have been shown to stimulate PRCA progression.[19,20] Histological and biochemical changes have been observed in tumor stroma.[9] Tumor stroma is commonly referred to as desmoplasia or reactive stroma. Stromal changes associated with carcinogenesis include loss of stromal protease inhibitors, altered ratio of stroma to epithelium, increased growth factor bioavailability, increased vimentin-positive cells, influx of inflammatory cells, increased protease activity and increased angiogenesis.[21,22]

Currently, there is a lack of information on how human prostatic epithelial cells progress from benign to malignant. This is in part due to the lack of models for evaluating human PRCA progression. We have previously reported that coadministration of T+E_2 stimulates cancer progression and malignant transformation in rat urogenital mesenchyme (rUGM) + BPH-1 TRs.[3,23] This model does not incorporate highly mutagenic agents or over-expression of oncogenes to induce carcinogenesis or malignant transformation. Instead, circulating sex steroids and stromal cells are used to transform nontumorigenic epithelial cells into malignant carcinomas.

Currently, this is the only model in which human prostatic cancer progression occurs with compounds found naturally in both rodents and humans. To better understand stromal–epithelial interactions in prostate carcinogenesis in this model, substitution of rUGM with genetically modified mouse urogenital mesenchyme (mUGM) would permit examination of specific stromal *versus* epithelial contributions to the carcinogenic process. The objectives of the present study were to determine the plasma levels of T and E_2 necessary to elicit human PRCA progression *in vivo* and to determine whether [T+E_2]-treatment can induce cancer progression and metastases in mUGM+BPH-1 TRs. Validation of the ability of mUGM to promote PRCA progression in the UGM+BPH-1 model will allow the use of UGM from genetically altered mice in future studies to evaluate the role of specific stromal genes in malignant progression and metastases, and will facilitate investigation of the hormonal and stromal mechanism(s) regulating PRCA. The model presented herein is the first and only demonstration of experiment progression of a nontumorigenic human epithelial cell to tumorigenesis and hence to metastasis in response to natural agents within the stromal microenvironment.

Material and methods

Steroid implants and collection of plasma

All animals and animal procedures were used in accordance with regulations approved by the University of California San Francisco's animal care committee. Silastic implants contained differing amounts of T or E_2 to generate ratios of T (mg):E_2 (mg) of 100:10, 25:2.5, 2.5:0.25, 25:0.25, 25:0, 2.5:2.5 and 0:2.5 (n = 8/dose). Intracardiac punctures were performed utilizing heparinized syringes. One milliliter of blood was collected and kept on ice for 1 hr. Samples were then centrifuged at 12,000g for 10 min, and plasma was collected and stored at -20^oC until analyses for T and E_2 could be performed.

Measurement of sex steroids

Assays measure both free and bound T or E_2 in plasma. Plasma (n = 5/group) levels of T and E_2 were analyzed by ELISA (Alpco, Windham, NH) as described by the manufacturer's protocol.

Preparation and processing of grafts

Pregnant CD-1 mice were obtained from Charles River (Wilmington, MA), and enhanced green fluorescent protein transgenic mice and Fc receptor, IgG, low affinity III (Fcgr3)-deficient mice were purchased from Jackson Laboratory. TRs were prepared and grafted under the renal capsule of male athymic nude mice as described previously[3,23] (see: http://mammary.nih.gov/tools/Cunha001/index.html). Animals were housed in the UCSF laboratory animal resource center with food and drinking water *ad libitum* under controlled conditions (12hr light, 12 hr dark; (20 ± 2)°C).

Tissue collection

Hosts were euthanized by CO_2 inhalation followed by cervical dislocation. Collections of renal lymph nodes were performed prior to removal of kidneys. Kidneys were excised, and grafts were dissected free of host kidney, weighed and processed for immunohistochemistry and cell culture. A subset of grafts was left intact on the kidney to evaluate invasion by histopathology.

Isolation of cell strains

mUGM+BPH-1 grafts from untreated and [T+E_2]-treated hosts were cut into small fragments (1–2 mm³) and cultured *in vitro*. Epithelial cells were isolated in culture as described previously.[23] Tissue fragments were cultured overnight in 4-well plates with 200 ml of tissue culture medium (RPMI 1640 containing 5% FBS). The following day, medium and any unattached fragments were aspirated and replaced with 200 µl of fresh medium every 3rd day. After 2 weeks, the medium was supplemented with 500 µg/ml G418 (Clontech, Palo Alto, CA). G418 selection was applied for

2 weeks. The resulting neomycin-resistant T-antigen (TAg)- and cytokeratin-positive cell populations were expanded in culture and used for regrafting experiments.

Regrafting experiments

Epithelial cells (100,000) of each of the derived cell strains were suspended in 50 µl of rat tail collagen gel as described and grafted under the renal capsules or subcutaneously in intact or castrated male athymic mice. After 1–2 months of growth, hosts were euthanized, lymph nodes were collected and the grafts were removed from the kidney. Grafts were weighed, fixed in 10% formalin and processed for histology.

Immunohistochemistry

Immunohistochemical procedures were performed as described previously.[3] Briefly, antigen retrieval for all antibodies except CD31 was performed by boiling slides in 20 mM citrate buffer (Vector, Burlingame, CA) for 30 min in a microwave oven. Nonspecific binding sites were blocked with a 1.5% (v:v) dilution of appropriate normal serum in PBS (pH 7.4) or in superblock (Immunovision technology Co., South San Francisco). For detection of CD31, preincubation of slides in 0.25% trypsin solution prior to addition of blocking solution was necessary. Each sample was subsequently treated with specific antibodies against smooth muscle α-actin (Sigma, St. Louis, MO; 1:500), vimentin (Chemicon, Temecula, CA; 1:200), CD31 (Pharmingen, San Diego, CA; 1:300), E-cadherin (E-cad; Transduction Laboratories, San Diego, CA; 1:250), Ki67 (Immunotech, Westbrook, ME; 1:100), cytokeratin-10 (Dako, Carpinteria, CA; 1:100), cytokeratins-8 (LE41), -14 (LE61; gift from Dr. E.B. Lane, University of Dundee, Scotland, UK; 1:5), chromogranin A (Dia Sorin, Stillwater, MN; 1:500), synaptophysin (Chemicon; 1:100) and Nkx3.1 (Zymed labs, South San Francisco; 1:50). Negative controls consisted of substitution of primary antibodies with the nonimmune IgG. Incubation with specific antibodies or their respective controls was carried out at 4^oC for 1 hr in a humidified chamber. After incubation with the secondary antibody, sections were washed in PBS (2 × 5 min washes) and incubated with avidin–biotin complex (Vector Laboratories) for 30 min at room temperature. After an additional 10 min of washing in PBS, immunoreactivity was visualized using 3,3′-diaminobenzidine in PBS and 0.3% H_2O_2. Sections were counterstained with hematoxylin.

For detection of SV40 T-antigen (Santa Cruz Biotechnology, Santa Cruz, CA; 1:250), the immunohistochemistry protocol was modified. Biotinylated primary antibodies were substituted for primary antibody alone. Antibodies were biotinylated according to kit instructions (Dako, Carpinteria, CA). Biotinylated antibodies were applied to slides for 30 min. After rinsing with PBS, streptavidin-peroxidase was added for 15 min. Slides were stained with DAB and counterstained with hematoxylin.

Growth indices

Proliferation and cell death indices were determined as described previously.[3]

Determination of cancer incidence

Paraffin sections were mounted on microscope slides. Sections were scored for presence or absence of malignant histopathology. Malignancy was defined using both cytologic and architectural criteria. Cytologic features of malignancy included nuclear enlargement (nuclei >2× normal), nuclear pleomorphism (2× nuclear variability within groups), nuclear hyperchromasia, nuclear contour irregularity and presence of macronucleoli. Architectural criteria for malignancy were characterized by haphazardly arranged small to medium sized glandular structures, and angulated and irregular tumor nests and trabeculae demonstrating destructive invasive growth. Invasion was defined by infiltrative growth into normal adjacent host kidney or into capsular fibrous tissue with desmoplastic tissue reaction. Glands demonstrating cytologic fea-
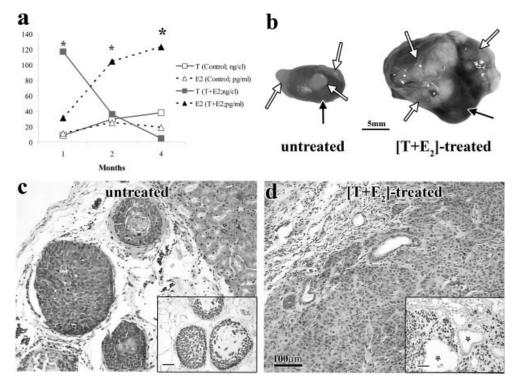
FIGURE 1 – Evaluation of plasma steroids and mUGM+BPH-1 cell TRs in steroid implanted and untreated nude mice. Silastic capsules containing 25 mg of T and 2.5 mg of estrogen (E_2) were implanted subcutaneously in nude mice. Plasma T and E_2 concentrations were determined by ELISA. (a) Plasma T levels were significantly ($*p < 0.01$) increased at 1 month and declined to normal levels at 2 and 4 months, whereas E_2 levels were at normal levels at 1 month and were significantly elevated at 2 and 4 months. (b) mUGM + BPH-1 TRs (white arrows) grown on the kidney (black arrows) in untreated and [T+E_2]-treated nude mouse hosts. Whole mounts of mUGM+BPH-1 grafts from untreated hosts show a modest amount of growth and lack of invasion, whereas [T+E_2]-treated hosts developed large bulky tumors that were highly vascularized and invasive. Hematoxylin and eosin staining of mUGM+BPH-1 TRs from (c) untreated and (d) [T+E_2]-implanted hosts. mUGM+BPH-1 TRs grown in untreated hosts exhibit orderly benign architecture (c), whereas in [T+E_2]-treatment hosts, the histopathology was indicative on carcinoma (note glandular structures, asterisks) (d). Insets demonstrate imunolocalization of large T-antigen (TAg) in mUGM+BPH-1 TRs from (c) untreated and (d) [T+E_2]-treated mice. Nuclear localization of TAg verifies the authenticity of human BPH-1 cells (see methods). In untreated specimens, TAg-positive cells were always surrounded by thick stroma indicative of normal developing prostate. Invasive TAg-positive carcinoma cells can be seen surrounding kidney tubules (*) in mUGM+BPH-1 grown in [T+E_2]-treated hosts.

TABLE I – CANCER INCIDENCE, MASS, AND GROWTH OF MOUSE UGM+BPH-1 TISSUE RECOMBINANTS GROWN IN ATHYMIC NUDE MOUSE HOSTS WITH OR WITHOUT [T + E_2] IMPLANTS FOR 4 MONTHS

Graft type	Treatment	Recovery of grafts	Cancer incidence	Mass (mg)	Ki67-index (%)	TUNEL-index (%)
Mouse UGM+BPH-1	Untreated	59/74 (79.7%)	1/59 (1.7%)	27.0 ± 1.6	8.5	0.8
	[T + E_2]	32/48 (66.7%)	28/32 (87.5%)*	191.2 ± 43.8*	30.1*	4.3*
Rat UGM+BPH-1	Untreated	6/8 (75%)	0/6 (0)	29.7 ± 4.8	12.3	0.4
	[T + E_2]	5/8 (62.5%)	5/5 (100%)*	187.2 ± 40.7*	33.1*	3.4*

*Significant difference at $p < 0.01$.

tures of malignancy but lacking features of destructive invasive growth were interpreted as dysplasia and not considered malignant.

Statistics

Data were analyzed by general linear models analysis of variance (SAS Institute, Cary, NC). When the F test was significant ($p < 0.05$), differences among means were evaluated by SNK post-test comparison or t tests (when appropriate).

Results

Plasma steroid levels

Plasma T levels for untreated mice were 0.9, 3.0 and 3.8 ng/ml vs. 11.7, 3.6 and 0.5 for [T+E_2] implanted mice at 1, 2 and 4 months after capsule implantation, respectively (Fig 1a). At 1 month, T was significantly ($p < 0.01$) higher than untreated levels. Plasma E_2 levels for untreated mice were 11.1, 25.6 and 19.2 pg/ml $versus$ 31.1, 104.5 and 122.8 pg/ml for [T+E_2]-treated mice at 1, 2 and 4 months after capsule implantation, respectively. Steroid implants significantly ($p < 0.01$) increased plasma levels of E_2 at 2 and 4 months.

Gross appearance of TRs

Grafts of either mUGM alone ($n = 8$) or BPH-1 cells alone ($n = 8$) in both untreated and treated mice were small (<5.0 mg), unorganized, and noninvasive (data not shown). In untreated mice, mUGM + BPH-1 TRs grafts were small (10–50 mg) and noninvasive when harvested 2 and 4 months after transplantation, regardless of whether the UGM was from wild-type mice (cd-1-strain; $n = 53$; Fig. 1b), enhanced GFP mice (FVB-strain; $n = 3$) or Fcgr3 mice (B6-strain; $n = 3$;). One mUGM+BPH-1 graft out of 59 total grafts was small (27.3 mg) but appeared to be cancer, as determined by histopathological analysis (Table I). In contrast, mUGM+BPH-1 TRs from [T+E_2]-treated mice were large, locally invasive and highly vascularized (Fig 1c). Average wet

TABLE II – THE EFFECTS DIFFERENT STEROID RATIOS AND PROSTATE CANCER PROGRESSION

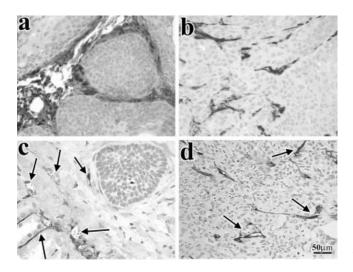| Treatment design	Testosterone (mg)	Estradiol (mg)	Result
Decreasing ratio	100	10	Cancer (8/8)
	25	2.5	Cancer (16/16)
	2.5	0.25	Benign (6/6)
Constant T, decreasing E$_2$	25	2.5	Cancer (8/8)
	25	0.25	Benign (8/8)
	25	0.0	Benign (7/7)
Decreasing T, constant E$_2$	25	2.5	Cancer (8/8)
	2.5	2.5	SQM (8/8)
	0.0	2.5	SQM (12/12)

SQM, squamous metaplasia.

FIGURE 2 – Identification of stromal cell types within mUGM + BPH-1 cell TRs from (*a* and *c*) untreated and (*b* and *d*) [T+E$_2$]-treated nude mice. Immunolocalization of smooth muscle α-actin (SMA) in mUGM+BPH-1 TRs from (*a*) untreated mice demonstrated thick smooth muscle sheets around the benign epithelium. In [T+E$_2$]-induced tumors (*b*), SMA is sporadically found and appears to be associated with the vasculature. Immunolocalization of CD31 (endothelial cell marker; arrows) in mUGM+BPH-1 TRs from (*c*) untreated and (*d*) [T+E$_2$]-treated mice. TRs from (*c*) untreated mice demonstrated CD31 in cells lining small blood vessels found exclusively within the stroma or within the kidney, whereas in (*d*) [T+E$_2$]-induced tumors, the vasculature consists of small fibro-vascular vessels densely localized throughout the carcinoma. Vimentin-positive cells were rarely observed in mUGM+ BPH-1 TRs from untreated mice, whereas they were intermingled throughout the tumor in mUGM+BPH-1 TRs collected from [T+E$_2$]-treated mice (not illustrated).

weight of [T+E$_2$]-treated TRs was 191.2 mg *versus* 27.0 mg in untreated mUGM+BPH-1 TRs (Table I). Additionally, [T+E$_2$]-treated mUGM+BPH-1 TRs had a significantly ($p < 0.001$) higher cancer incidence (87.5%) as determined by histopathology compared to the untreated group (1.7%).

To determine if mUGM+BPH-1 TRs behaved differently than rUGM+BPH-1 TRs, a side by side comparison was performed. The two groups were similar in cancer incidence, histopathology, tissue growth and mass when grown in either untreated or [T+E$_2$]-treated hosts (Table I). Evaluation of varied doses of [T+E$_2$] lead to histopathology of either cancerous or nontumorigenic tissues (data not shown). Only the groups containing T:E$_2$ ratios of 25:2.5 and 100:10 elicited carcinogenesis. Groups containing T:E$_2$ ratios of 0:2.5 and 2.5:2.5 developed benign squamous metaplasia as judged by histopathology. All other groups (2.5:0.25, 25:0.25 and 25:0) evaluated showed a benign histopathology similar to that of the control untreated groups (data not shown) (Table II).

Histology

mUGM + BPH-1 grafts grown in intact untreated male hosts contained a well organized, differentiated noninvasive epithelium (Fig. 1*c*). The epithelium consisted of benign solid and canalized ductal structures surrounded by a thick smooth muscle stroma. All epithelial structures were immuno-positive for TAg (Fig. 1*c* inset). In no case were invasive TAg positive cells found within the stroma of mUGM + BPH-1 grafts grown in untreated male hosts. The stroma consisted predominantly of smooth muscle α-actin-positive cells (Fig. 2*a*) and some interspersed vimentin-positive cells (not illustrated). Additionally, CD31-positive vascular profiles were observed within the stroma only (Fig. 2*c*).

When mUGM + BPH-1 grafts were grown in [T+E$_2$]-treated male hosts for four months, 87.5% of grafts underwent carcinogenesis as determined by histopathological evaluation (Table I). Such [T+E$_2$]-treated mUGM + BPH-1 grafts were characterized by the lack of both epithelial and stromal organization. Tongues of invasive epithelial cells were seen invading the host's kidney (Fig. 1*d*). The abnormal epithelium was TAg-positive (Fig. 1*d*). Localization of SMA was dramatically reduced in tumorigenic mUGM + BPH-1 TRs compared to untreated TRs (Fig. 2*b*). When SMA-positive cells were found in [T+E$_2$]-treated mUGM + BPH-1 TRs, they appeared to be associated with the vasculature as opposed to encircling epithelial structures. Localization of CD31-positive cells lining vascular profiles were markedly increased in [T+E$_2$]-treated mUGM + BPH-1 TRs *versus* untreated mUGM + BPH-1 TRs (Fig. 2*d*). These tumors exhibited invasive squamous, basal, and adeno-carcinoma phenotypes as determined by histopathology. Tumors exhibited high-grade malignant cytological features including nuclear pleomorphism, anisonucleosis, nuclear hyperchromasia, nucleolar enlargement, numerous mitotic figures and abnormal mitoses (Fig. 1*d*).

Localization of epithelial differentiation markers

Antibodies to cytokeratins (CK)-8, -10 and -14 were used to assess differentiation markers indicative of luminal cells, cornified cells and basal cells, respectively. Both luminal (CK-8) and basal cell markers (CK-14) were expressed in all mUGM+BPH-1 TRs from either untreated and [T+E$_2$]-treated animals. CK-10, a marker of cornification, was associated with stratified squamous epithelial cells and squamous carcinoma cells (Fig. 6), which were heterogeneously distributed in most mUGM+BPH-1 [T+E$_2$]-induced tumors.

Proliferation index

Localization of nuclear Ki67 was used to evaluate proliferation in both untreated and [T+E$_2$]-treated mUGM+BPH-1 TRs and rUGM+BPH-1 TRs. On the basis of the counting of more than 8,500 individual nuclei per group, the Ki67 labeling index averaged 8.5% in mUGM+BPH-1 TRs grown in untreated male hosts and 30.1% in mUGM+BPH-1 TRs grown in [T+E$_2$]-treated hosts (Table I). For rUGM+BPH-1 TRs, Ki67 epithelial labeling index averaged 12.3% in rUGM+BPH-1TRs grown in untreated male hosts and 33.1% in rUGM+BPH-1 TRs grown in [T+E$_2$]-treated hosts. Proliferative activity was significantly higher ($p < 0.01$) in UGM+BPH-1 TRs grown in hosts treated with [T+E$_2$] as compared with untreated hosts.

Cell death index

Determination of TUNEL-positive cells was used to evaluate cell death in both untreated and [T+E$_2$]-treated mUGM+BPH-1 and rUGM+BPH-1 TRs. Epithelial TUNEL-labeling index averaged 0.8% in mUGM+BPH-1 TRs grown in untreated male hosts and 4.3% in mUGM+BPH-1 TRs grown in [T+E$_2$]-treated hosts (Table I). For rUGM+BPH-1 TRs, the TUNEL-labeling index averaged 0.4% in rUGM+BPH-1 TRs grown in untreated male hosts and 3.4% in rUGM+BPH-1 TRs grown in [T+E$_2$]-treated hosts. Cell death was significantly higher ($p < 0.01$) in UGM+BPH-1 TRs grown in hosts treated with [T+E$_2$] as compared with untreated hosts.

Determination of metastases

Distant organ metastases were identified visually in 2/25 mice that were treated with T+E2 and were grafted with mUGM+BPH-1 TRs. Liver and lung metastases were identified by their large nodular discolored growths within the respective organs (Fig. 3a). Renal lymph nodes from untreated and [T+E$_2$]-treated mice bearing mUGM+BPH-1 TRs differed in appearance at 16 weeks. Renal lymph nodes isolated from [T+E$_2$]-treated mice contralateral to the tumor or lymph nodes collected from untreated mice with mUGM+BPH-1 TRs were whitish, 2–3 mm in size (8/8 mice; Fig. 3b left) and were thus similar in appearance and size to those of normal mice. In contrast, lymph nodes ipsilateral to mUGM+BPH-1 tumors in [T+E$_2$]-treated animals were reddish and 4–5 mm in size (3/8 mice; Fig. 3b right). Histologically, lymph nodes ipsilateral to tumors in [T+E$_2$]-treated mice were disorganized and contained few germinal centers. Many cells within the lymph nodes of tumor bearing [T+E$_2$]-treated hosts were positive for TAg (Fig. 3c). Lymph nodes from both untreated and contralateral to tumors were normal, contained germinal centers and were negative for TAg (Fig. 3c right).

Determination of malignant transformation

To confirm that the histopathological diagnosis of cancer was consistent with independent malignant growth, we tested the ability of cells isolated from mUGM+BPH-1 grafts from untreated and [T+E$_2$]-treated hosts to grow independent of [T+E$_2$]-stimulation and stromal contributions. BPH-1 cells contain a neomycin resistance gene which flanks the large T-antigen cDNA. After isolating epithelial cells from mUGM+BPH-1 TRs using the G418 selection, 4 cell strains were derived from mUGM+BPH- 1+ [T+E$_2$] tumors (designated WAR-1, 2, 3 and 4), and an additional three epithelial strains were derived from untreated benign mUGM+BPH-1 TRs (designated WAR-100, 101 and 102). When grown on plastic, the cell strains derived from untreated TRs (WAR-100–102) had a typical epithelial cobblestone morphology. [T+E$_2$]-induced tumor derived BPH-1 cells (WAR-1–4) also had an epithelial cobblestone

morphology but were generally less tightly adherent to the tissue culture flask (in the presence of 0.05% trypsin) compared to tightly adherent BPH-1 cells isolated from untreated mUGM+BPH-1 TRs (WAR-100–102) or parental BPH-1 cells.

Cells isolated from both groups were grafted to the kidney or subcutaneous sites of intact or castrated male athymic mouse hosts. WAR-100 cells derived from untreated mUGM+BPH-1 TRs never formed tumors, regardless of graft site or hormonal milieu (0/48; Fig. 4a and 4c). In contrast, epithelial cells derived from all [T+E$_2$]-treated mUGM+BPH-1 TRs (WAR-1–4) grew rapidly as tumors in either graft site in both intact or castrated hosts (64/64; Fig. 4a and 4c). In all cases nontumorigenic or tumorigenic grafts were positive for TAg (Fig. 4c insets), verifying the BPH-1 origin of the cells. Grossly, the tumors grew at a variety of rates but typically engulfed and destroyed the host kidney given sufficient time. Tumors derived from tumorigenic [T+E$_2$]-induced BPH-1 cells (WAR-1–4) were histologically squamoid or adenosquamous (Fig. 4c, middle), similar to primary mUGM+BPH-1 TRs tumors from which they were derived. Some tumors grew as noninvasive proliferative lesions, whereas others were locally invasive and metastatic. When WAR-1 cells were grown on kidneys for 2 months, ipsilateral renal lymph nodes contained metastatic cells (3/10; Fig. 4a, right). These metastatic cells were TAg-positive (Fig. 4c right inset), and thus verify authenticity of the BPH-1 cells.

Identification of progression markers

In mUGM+BPH-1 TRs grown in untreated hosts, E-cad was associated with the epithelial cell membranes (Fig. 5a left). In mUGM+BPH-1 T+E$_2$-induced primary tumors or metastases, intensity of E-cad localization was dramatically reduced, diffuse or entirely absent (Fig. 5a middle and right). Nkx3.1 was localized to the cytoplasm and nuclei in untreated mUGM+BPH-1 TRs (Fig. 5b left). Tumors developing from mUGM+BPH-1 TRs grown in [T+E$_2$]-treated mice were mostly devoid of Nkx3.1 staining, however, 2/3 lymph node metastases demonstrated increased cyto-
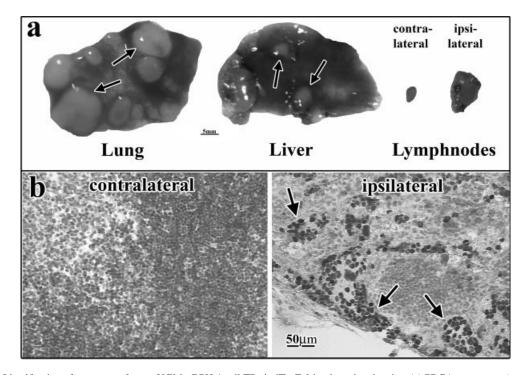

FIGURE 3 – Identification of metastases from mUGM+BPH-1 cell TRs in [T+E$_2$]-implanted nude mice. (a) PRCA metastases (arrows) to lung and liver of mice with mUGM+BPH-1 TRs in [T+E$_2$]-implanted nude mice. (b) Renal lymph nodes contralateral to [T+E$_2$]-induced tumors (left) were small and whitish in appearance. Renal lymph nodes ipsilateral (right) to mUGM+BPH-1 grafts collected from [T+E$_2$]-implanted mice were larger and highly vascularized. TAg-positive cells were observed in lymph nodes from [T+E$_2$]-treated mice (c; arrows) and not in LNs from untreated mice.
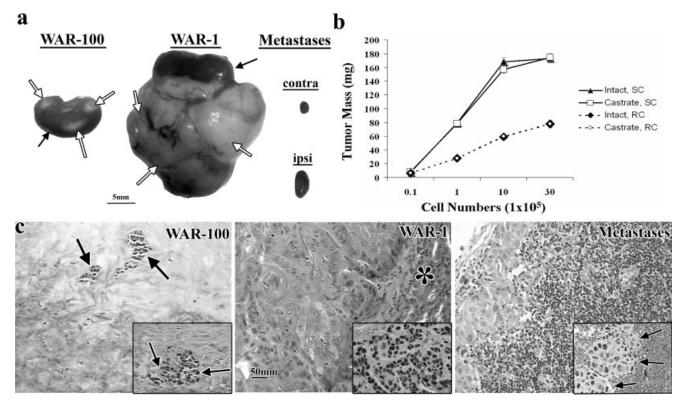
FIGURE 4 – Malignant transformation occurs in mUGM+BPH-1 cell TRs from [T+E₂]-treated hosts, but not from untreated hosts. mUGM+BPH-1 TRs were grown in mice for 4 months in either untreated or [T+E₂]-treated nude mouse hosts. Grafts were excised, minced and grown on plastic. Isolation of BPH-1 epithelial cells was achieved by incubating the cultures with G418. After BPH-1 cells were isolated from untreated TRs (WAR-100–102) or [T+E₂]-treated (WAR-1–4) TRs, they were regrafted (100,000 cells/graft) subcutaneously or under the renal capsule of either castrate or intact nude mouse hosts and grown for 1–2 months without stromal cells or steroid implants. Note the large invasive tumors produced by WAR-1 cells, whereas WAR-100s were small and noninvasive (*a*). Renal lymph nodes contained metastases only when ipsilateral to WAR-1 tumors (but not WAR-100 grafts or contralateral to tumors) and were large (~5 mm) in size. Growth rates of WAR-1 were determined in different hormonal milieus, at different cell concentrations and in different anatomical sites. WAR-1 cells (1×10^5, 1×10^5, 1×10^6 and 3×10^6 cells/graft) were grafted subcutaneously (SC) or under the renal capsule (RC) into castrate or intact nude mouse hosts and grown for 28 days (*b*). WAR-100 cells survived equally well in intact or castrated male hosts; however, mass of WAR-100 grafts exhibiting benign architecture were much smaller (<10 mg; not illustrated). There were no significant differences between WAR-1 and WAR-100 graft mass grown in castrate or intact hosts. H&E staining of WAR-100 and WAR-1 grafts (*c*, left) demonstrates the lack of growth and malignant transformation in WAR-100 cells derived from untreated TRs (*c*). WAR-100 cells are undifferentiated and lack organized epithelial structures. WAR-1 cells derived from untreated [T+E₂]-induced tumors (*c*, middle) contained squamoid and adenosquamous carcinomatous features (note glandular structures, asterisks). Immunolocalization of TAg in (*e*) WAR-100 and (*f*) WAR-1 grafts verifies their BPH-1 origin. (*c*, right) Histological analysis of renal lymph nodes located ipsilateral to WAR-1 grafts grown for 2 months in nude mouse hosts. Renal lymph nodes ipsilateral to WAR-100 grafts were small and whitish in appearance. Metastatic lymph nodes were highly vascularized and contained TAg-positive cells (*c*, right) whereas, renal lymph nodes ipsilateral to benign WAR-100 grafts were negative for TAg (not illustrated).

plasmic, but not nuclear, expression of Nkx3.1 protein (Fig. 5*b* right). The phosphorylated form of pAkt was not detected in nontumorigenic mUGM+BPH-1 TRs grown in untreated hosts (Fig 5*c* left), but marked cell membrane and cytoplasmic localization was observed in regions of tumorigenic mUGM+BPH-1 grafts grown in [T+E₂]-treated hosts (Fig. 5*c* middle). pAkt localization was also observed in 2/3 primary lymph node metastases (Fig. 5*c* right).

Discussion

The present study demonstrates that immortalized nontumorigenic human prostatic epithelial cells progress to full tumorigenesis when recombined with mUGM and grown in [T+E₂]-treated hosts. This progression occurred at a high incidence (87.5%). We have previously demonstrated that rat UGM+BPH-1 TRs also progress from benign to cancerous lesions under similar conditions.[3] One important difference observed in this study was metastases to renal lymph nodes and distant organs. Wang and colleagues (2001), who reported [T+E₂]-induced tumorigenic progression in rat UGM+BPH-1 TRs, did not evaluate metastases in their model. Cumulatively, both models demonstrate the impor-

tance of stroma and steroid hormones in the progression of nontumorigenic BPH-1 cells to tumorigenesis and metastases.

Our definition of "nontumorigenicity" of the parental BPH-1 cell is particularly rigorous. We define nontumorigenicity as the absence of tumors in grafts of parental BPH-1 cells or BPH-1 cells isolated TRs in untreated control animals even though living BPH-1 cells were detected in the graft site at the end of the experiment (3–12 months post-grafting) by SV40-Tag staining. Over the years of using the BPH-1 model, we have detected 2 tumors in 578 control grafts. These 2 tumors were small and demonstrated an intimate association of epithelial profiles having benign and carcinomatous features. The close association of benign and carcinomatous histopathology suggests that the parental nontumorigenic BPH-1 cells cannot inhibit growth of tumorigenic variants *via* paracrine factors. We know that the tumorigenic BPH-1 cells developing in UGM+BPH-1+[T+E₂] TRs are fast growing having doubling times of 2–8 days. If such tumorigenic cells were present in the original low passage clonally-derived parental nontumorigenic BPH-1 population (even at an incidence of 1/100,000 cells), sizable tumors would have been detected at high frequency in the BPH-1 control grafts grown for 3–12 months.
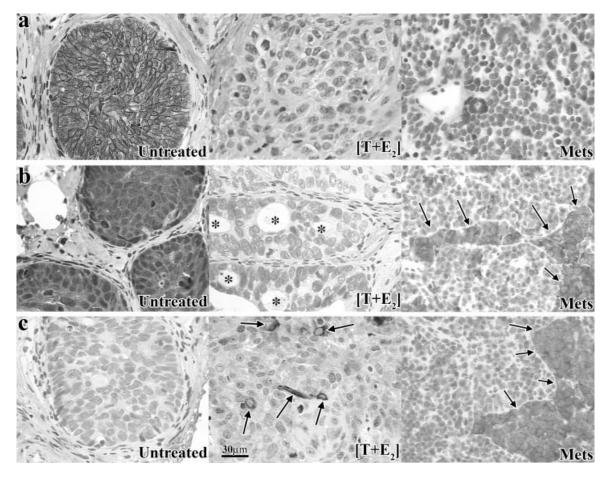
FIGURE 5 – Identification of PRCA progression markers E-cad, Nkx3.1 and phospho-Akt in mUGM+BPH-1 cells TRs (TRs). Immunolocalization of E-cad in mUGM+BPH-1 TRs from (*a*) untreated mice, [T+E$_2$]-treated primary tumors and metastases from primary tumors. In untreated TRs, E-cad was associated with the cell membranes. In tumorigenic mUGM+BPH-1 TRs and metastases, E-cad expression is decreased, diffused or undetectable. (*b*) Immunolocalization of Nkx3.1 in mUGM+BPH-1 TRs from untreated mice, [T+E$_2$]-treated tumors and primary metastases. Nkx3.1 is localized to both cytoplasm and nuclei of mUGM+BPH-1 TRs from untreated mice. Loss of Nkx3.1 expression is associated with PRCA progression in mUGM+BPH-1 TRs from [T+E$_2$]-treatment hosts (note glandular architecture, asterisks). Localization of Nkx3.1 increases (2/3 lymph nodes) within the cytoplasm of primary metastases. (*c*) Immunolocalization of phospho-Akt in mUGM+BPH-1 TRs from untreated mice, [T+E$_2$]-treated primary tumors and metastases from primary tumors. Phospho-Akt-positive cells were not found in mUGM+BPH-1 TRs from untreated mice. Phospho-Akt was localized to a subset of cells in [T+E$_2$]-induced tumors and to the lymph node metastases (2/3 lymph nodes).

Sex steroids play a key role in PRCA-progression. T+E$_2$ act synergistically in rodents to induce PRCA.[2,4] As men age serum levels of T decrease as E$_2$ levels increase, it causes an overall increase in the ratio of E$_2$ to T. In this study, [T+E$_2$]-implanted mice have serum T and E$_2$ levels that are approximately 2–3 times higher than those found in middle aged men.[24,25] Moreover, levels of T decrease in the murine hosts as plasma levels of E$_2$ increase, similarly to what occurs in aging men. These steroid levels provide a near physiologic but carcinogenic hormonal milieu that acts upon both stromal and epithelial compartments to induce carcinogenesis in initiated but nontumorigenic human prostatic epithelial cells.

Human PRCA usually contains a heterogeneous mixture of precancerous (PIN) and cancerous lesions expressing luminal cell markers. Within human prostate tumors, it is common to see high grade invasive cancer mixed with benign glands as well as a range of histopathologies between these two extremes. Our model uses nontumorigenic human prostatic BPH-1 epithelial cells, which *in vitro* express cytokeratins diagnostic for luminal cells.[26] When recombined with mouse UGM and grown in untreated male hosts, the epithelium expresses morphological and biochemical features reminiscent of developing prostate. The BPH-1 cells in combination with mUGM form solid and canalized cords of Nkx3.1-positive cells that in some cases form ductal structures. Moreover, in

untreated UGM+BPH-1 recombinants, the epithelium expressed the luminal cell marker (CK-8), the basal cell marker (CK-14) and the squamous marker (CK-10). Expression of CK-14 seen in untreated and [T+E$_2$]-treated mUGM+BPH-1 TRs was not observed in the original report on BPH-1 cells growing *in vitro*.[26] Presumably, the more favorable growth and morphogenetic conditions afforded *in vivo* in combination with mUGM allows for expression of a broader spectrum of differentiation markers. In any case, the expression of both luminal and basal epithelial markers in mUGM+BPH-1 TRs reveals a broad developmental potential of BPH-1 cells as well as the heterogeneity of cell differentiation typically found within developing prostate.[27] For example, in the neonatal period, distal ducts of developing rat prostates are solid, and the epithelial cells coexpress both luminal and basal cell markers. In contrast, canalized proximal ducts contain distinct luminal and basal cells each expressing their characteristic set of differentiation markers.[27] Functionally, mUGM+BPH-1 TRs respond accordingly to E2 administration only by undergoing squamous metaplasia (see Table II). Notably, BPH-1 cells in any context (*in vitro, in vivo*, with or without UGM) do not express neuroendocrine markers, synaptophysin A or chromogranin A.

The tumors developing in UGM+BPH-1 recombinants treated with T+E$_2$ were composed primarily of squamous carcinoma and to
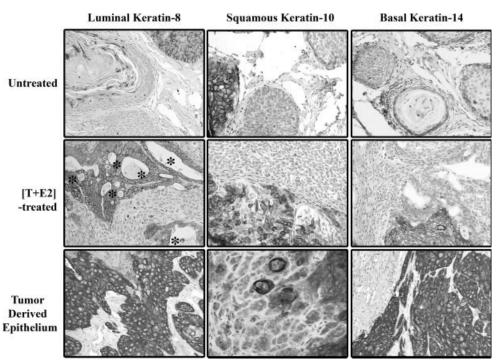
FIGURE 6 – Localization of cytokeratins in mUGM+BPH-1 cell TRs in control untreated and [T+E₂]-implanted nude mice. (*a*) Localization of luminal-, squamous- and basal-cell markers cytokeratin-8, -10 and -14 (respectively) within control untreated TRs. (*b*) Localization of Adeno-, squamous- and basal-carcinoma markers cytokeratin-8, -10 and -14 (respectively) within [T+E₂]-treated TRs (note glandular architecture in cytokeratin-8 positive cells, asterisks).

a lesser extent basal and adenocarcinoma. Presumably this heterogeneity is due to the plasticity of BPH-1 cells and the hormonal milieu. As mentioned above, BPH-1 cells produce keratins-8 and -14 *in vivo* when combined with UGM and grown in untreated or T+E₂ treated hosts. Keratin-8 and -14 are markers indicative of adenocarcinomas and basal cell carcinomas (respectively; see Fig. 6). The preponderance of squamous cancer is presumably due to the estrogenic environment caused by the E₂ implants.

Tumor growth and development are dependent upon a rich vascular bed. For several transgenic mouse models of tumorigenesis, the so-called ''vascular switch'' to high vessel density is a critical step in progression from benign to tumorigenic growth.[28,29] In the mUGM+BPH-1 model, vascular density changes quantitatively and qualitatively as one would expect during hormone-induced carcinogenic progression. mUGM+BPH-1 TRs grown in untreated hosts develop benign epithelial architecture and have a low vascular density confined to stroma surrounding the epithelium. However, during [T+E₂]-induced carcinogenesis in mUGM+BPH-1 TRs, blood vessels infiltrate deeply into the malignant epithelium at high density. The increased vascularity during PRCA progression in this model is not only consistent with prostate carcinogenesis but may provide a unique model in which to study angiogenesis during carcinogenesis.

Models of PRCA development are designed to mimic certain aspects of the disease process, which in humans occurs over a period of many years. A variety of transgenic models have been described based upon the targeting of oncogenes to the prostate[30–32] or the deletion of tumor suppressor genes.[2,33,34] Each of these models has been useful for studying various aspects of prostatic carcinogenesis, the progression from benign to tumorigenic and metastatic growth. A major question regarding animal models of prostatic carcinogenesis is their relevance to human disease. A unique feature of the rUGM+BPH-1[3] and the mUGM+BPH-1 models is that progression occurs in initiated but nontumorigenic human prostatic epithelial cells. The mUGM+BPH-1 model is the only model in which human prostatic epithelial cells progress

from benign to tumorigenic and hence to metastatic growth. Most importantly, progression from benign to metastatic growth occurs within 16 weeks. Progression in the mUGM+BPH-1 model described herein has been characterized by histopathological criteria, tumor size (mass) and associated changes in expression of gene products (Nkx3.1, pAkt and E-cad). All of these epithelial markers are expressed appropriately in untreated mUGM+BPH-1 TRs in a fashion comparable to that in normal human prostate. These markers show aberrant expression in mUGM+BPH-1 TRs from [T+E₂]-treated hosts. Finally, transplantation studies have verified that changes in histopathology and marker expression are indeed coupled to tumor growth and transplantability independent of hormonal and stromal conditions. Using neomycin analogues to select and purify BPH-1 epithelial cells, untreated mUGM+BPH-1 TRs yielded BPH-1 (WAR-100–102) cells that exhibited benign growth, whereas [T+E₂]-induced primary mUGM+BPH-1 tumors yielded cells (WAR-1–4) that exhibited tumorigenic growth and metastases. In future studies, it should be possible to generate lineage-matched sets of BPH-1 cells (control nontumorigenic, tumorigenic and metastatic) from the same TRs. Such matched sets of BPH-1 cells will be the basis of assessing the earliest genetic, RNA and protein changes during progression from nontumorigenic to tumorigenic and tumorigenic to metastatic growth.

In this model, the nontumorigenic BPH-1 epithelial cells progress to form carcinomas and develop metastases to the adjacent renal lymph nodes and to distant organs. The relevance to human PRCA is similar in that lymph node metastatses are a common site of metastatic spread in humans. Although 2/25 mice exhibited liver and lung metastases, determination of bone metastases was not evaluated. Future experiments will test the ability of these cells to metastasize to bone, especially in hosts that also receive grafts of human bone.[35]

In summary, we have developed a unique model for PRCA-progression that incorporates both the power of mouse genetics and human prostatic epithelial cells. This model recapitulates many

critical aspects of human prostatic carcinogenesis including metastases. We have also demonstrated that the combination of epithelium, stroma and hormonal milieu are all required for PRCA-progression, malignant transformation and metastases. New models that allow for therapeutic testing on human tissues as they progress to cancer may enhance the likelihood of determining the mechanisms of PRCA progression and finding a cure for PRCA in the future.

References

1. Wilson JD. The pathogenesis of benign prostatic hyperplasia. Am J Med 1980;68:745–56.
2. Wang Y, Hayward SW, Donjacour AA, Young P, Jacks T, Sage J, Dahiya R, Cardiff RD, Day ML, Cunha GR. Sex hormone-induced carcinogenesis in Rb-deficient prostate tissue. Cancer Res 2000;60: 6008–17.
3. Wang Y, Sudilovsky D, Zhang B, Haughney PC, Rosen MA, Wu DS, Cunha TJ, Dahiya R, Cunha GR, Hayward SW. A human prostatic epithelial model of hormonal carcinogenesis. Cancer Res 2001;61: 6064–72.
4. Noble RL. The development of prostatic adenocarcinoma in Nb rats following prolonged sex hormone administration. Cancer Res 1977; 37:1929–33.
5. Ouyang XS, Wang X, Lee DT, Tsao SW, Wong YC. Up-regulation of TRPM-2, MMP-7 and ID-1 during sex hormone-induced prostate carcinogenesis in the Noble rat. Carcinogenesis 2001;22:965–73.
6. Thompson CJ, Tam NN, Joyce JM, Leav I, Ho SM. Gene expression profiling of testosterone and estradiol-17 beta-induced prostatic dysplasia in Noble rats and response to the antiestrogen ICI 182,780. Endocrinology 2002;143:2093–105.
7. Bosland MC, Ford H, Horton L. Induction at high incidence of ductal prostate adenocarcinomas in NBL/Cr and Sprague-Dawley Hsd:SD rats treated with a combination of testosterone and estradiol-17 beta or diethylstilbestrol. Carcinogenesis 1995;16:1311–7.
8. Drago JR. The induction of NB rat prostatic carcinomas. Anticancer Res 1984;4:255–6.
9. Wang YZ, Cunha GR, Hayward SW. In vitro and in vivo models of prostate cancer. In: Carroll PR and Grossfeld GD, eds. American Cancer Society Atlas of Clinical Oncology. Hamilton, London: BC Decker Inc, 2002.68–81.
10. Risbridger G, Wang H, Young P, Kurita T, Wang YZ, Lubahn D, Gustafsson JA, Cunha G, Wong YZ. Evidence that epithelial and mesenchymal estrogen receptor-alpha mediates effects of estrogen on prostatic epithelium. Dev Biol 2001;229:432–42.
11. Couse JF, Lindzey J, Grandien K, Gustafsson JA, Korach KS. Tissue distribution and quantitative analysis of estrogen receptor-alpha (ERalpha) and estrogen receptor-beta (ERbeta) messenger ribonucleic acid in the wild-type and ERalpha-knockout mouse. Endocrinology 1997;138:4613–21.
12. Lau KM, Leav I, Ho SM. Rat estrogen receptor-alpha and -beta, and progesterone receptor mRNA expression in various prostatic lobes and microdissected normal and dysplastic epithelial tissues of the Noble rats. Endocrinology 1998;139:424–7.
13. Prins GS. Developmental estrogenization of the prostate gland. In: Naz RK, ed. Prostate: basic and clinical aspects. Boca Raton: CRC Press, 1997. 245–66.
14. Prins GS, Marmer M, Woodham C, Chang W, Kuiper G, Gustafsson JA, Birch L. Estrogen receptor-beta messenger ribonucleic acid ontogeny in the prostate of normal and neonatally estrogenized rats. Endocrinology 1998;139:874–83.
15. Leav I, Lau KM, Adams JY, McNeal JE, Taplin ME, Wang J, Singh H, Ho SM. Comparative studies of the estrogen receptors beta and alpha and the androgen receptor in normal human prostate glands, dysplasia, and in primary and metastatic carcinoma. Am J Pathol 2001;159:79–92.
16. Cunha GR, Lung B. The possible influences of temporal factors in androgenic responsiveness of urogenital tissue recombinants from wild-type and androgen-insensitive (Tfm) mice. J Exp Zool 1978;205:181–94.
17. Cunha GR, Donjacour AA, Cooke PS, Mee S, Bigsby RM, Higgins SJ, Sugimura Y. The endocrinology and developmental biology of the prostate. Endocr Rev 1987;8:338–62.
18. Donjacour AA, Rosales A, Higgins SJ, Cunha GR. Characterization of antibodies to androgen-dependent secretory proteins of the mouse dorsolateral prostate. Endocrinology 1990;126:1343–54.
19. Olumi AF, Grossfeld GD, Hayward SW, Carroll PR, Tlsty TD, Cunha GR. Carcinoma-associated fibroblasts direct tumor progression of initiated human prostatic epithelium. Cancer Res 1999;59: 5002–11.
20. Thompson TC, Truong LD, Timme TL, Kadmon D, McCune BK, Flanders KC, Scardino PT, Park SH. Transgenic models for the study of prostate cancer. Cancer 1993;71:1165–71.
21. McAlhany SJ, Ressler SJ, Larsen M, Tuxhorn JA, Yang F, Dang TD, Rowley DR. Promotion of angiogenesis by ps20 in the differential reactive stroma prostate cancer xenograft model. Cancer Res 2003;63: 5859–65.
22. Tuxhorn JA, Ayala GE, Rowley DR. Reactive stroma in prostate cancer progression. J Urol 2001;166:2472–83.
23. Hayward SWY, Cao M, Hom Y, Zhang B, Grossfeld G, Sudilovsky D, Cunha G. Malignant transformation in a non-tumorigenic human prostatic epithelial cell line. Cancer Res 2001;61:8135–42.
24. Belanger A, Candas B, Dupont A, Cusan L, Diamond P, Gomez JL, Labrie F. Changes in serum concentrations of conjugated and unconjugated steroids in 40- to 80-year-old men. J Clin Endocrinol Metab 1994;79:1086–90.
25. Fisher D, Nelson J. Endocrine testing and treatment, 4th ed, vol. 3. Philadelphia: W.B. Saunders, 2001.
26. Hayward SW, Dahiya R, Cunha GR, Bartek J, Deshpande N, Narayan P. Establishment and characterization of an immortalized but nontransformed human prostate epithelial cell line: BPH-1. In Vitro Cell Dev Biol Anim 1995;31:14–24.
27. Hayward S, Rosen M, Haughney P, Cunha G. The human prostatic epithelial cell line BPH-1 recapitulates some key events of human prostatic development in tissue recombinations with rat urogenital sinus mesenchyme. Prostate 1996;(Suppl 6):95.
28. Bergers G, Brekken R, McMahon G, Vu TH, Itoh T, Tamaki K, Tanzawa K, Thorpe P, Itohara S, Werb Z, Hanahan D. Matrix metalloproteinase-9 triggers the angiogenic switch during carcinogenesis. Nat Cell Biol 2000;2:737–44.
29. Coussens LM, Raymond WW, Bergers G, Laig-Webster M, Behrendtsen O, Werb Z, Caughey GH, Hanahan D. Inflammatory mast cells up-regulate angiogenesis during squamous epithelial carcinogenesis. Genes Dev 1999;13:1382–97.
30. Ellwood-Yen K, Graeber TG, Wongvipat J, Iruela-Arispe ML, Zhang J, Matusik R, Thomas GV, Sawyers CL. Myc-driven murine prostate cancer shares molecular features with human prostate tumors. Cancer Cell 2003;4:223–38.
31. Greenberg NM, DeMayo F, Finegold MJ, Medina D, Tilley WD, Aspinall JO, Cunha GR, Donjacour AA, Matusik RJ, Rosen JM. Prostate cancer in a transgenic mouse. Proc Natl Acad Sci USA 1995;92: 3439–43.
32. Kasper S, Sheppard PC, Yan Y, Pettigrew N, Borowsky AD, Prins GS, Dodd JG, Duckworth ML, Matusik RJ. Development, progression, and androgen-dependence of prostate tumors in probasin-large T antigen transgenic mice: a model for prostate cancer. Lab Invest 1998;78: 319–33.
33. Abate-Shen C, Banach-Petrosky WA, Sun X, Economides KD, Desai N, Gregg JP, Borowsky AD, Cardiff RD, Shen MM. Nkx3.1; Pten mutant mice develop invasive prostate adenocarcinoma and lymph node metastases. Cancer Res 2003;63:3886–90.
34. Wang SI, Parsons R, Ittmann M. Homozygous deletion of the PTEN tumor suppressor gene in a subset of prostate adenocarcinomas. Clin Cancer Res 1998;4:811–5.
35. Nemeth JA, Yousif R, Herzog M, Che M, Upadhyay J, Shekarriz B, Bhagat S, Mullins C, Fridman R, Cher ML. Matrix metalloproteinase activity, bone matrix turnover, and tumor cell proliferation in prostate cancer bone metastasis. J Natl Cancer Inst 2002;94:17–25.